

ICAR ATRP of Methyl Methacrylate Catalyzed by $\text{FeCl}_3 \cdot 6\text{H}_2\text{O}$ /Succinic Acid

Guoxiang Wang,¹ Mang Lu,² Yongbing Liu¹

¹College of Chemistry and Chemical Engineering, Hunan Institute of Science and Technology, Yueyang 414006, Hunan province, China

²School of Materials Science and Engineering, Jingdezhen Ceramic Institute, Jingdezhen 333001, Jiangxi Province, China

Received 6 July 2011; accepted 7 November 2011

DOI 10.1002/app.36448

Published online in Wiley Online Library (wileyonlinelibrary.com).

ABSTRACT: In this work, methyl methacrylate (MMA) was polymerized by initiator for continuous activator regeneration (ICAR) atom transfer radical polymerization (ATRP) method to obtain low molecular weight living polymers. The ATRP initiator was ethyl 2-bromoisobutyrate, the catalyst ligand complex system was $\text{FeCl}_3 \cdot 6\text{H}_2\text{O}$ /succinic acid, and the conventional radical initiator 2,2'-azobisisobutyronitrile was used as a thermal radical initiator. Polymers with controlled molecular weight were obtained with ppm level of Fe catalyst complex at 90°C in *N,N*-dimethylformamide. The polymer was characterized by nuclear magnetic resonance

(NMR). The molecular weight and molecular weight distribution of the obtained poly (methyl methacrylate) were measured by gel permeation chromatography method. The kinetics results indicated that ICAR ATRP of MMA was a "living"/controlled polymerization, corresponding to a linear increase of molecular weights with the increasing of monomer conversion and a relatively narrow polydispersities index. © 2012 Wiley Periodicals, Inc. *J Appl Polym Sci* 000: 000–000, 2012

Key words: polymer; nuclear magnetic resonance; living polymerization; catalyst

INTRODUCTION

Atom transfer radical polymerization (ATRP) is an effective technique of a living polymerization or a controlled/living radical polymerization to synthesize polymer with concise molecular weight and narrow molecular weight distribution. ATRP was independently discovered by many authors.^{1,2} In normal ATRP, an equilibrium was established between the active species and the dormant species via a reversible deactivation procedure. That is to say, the dormant alkyl halide (R-X) was reacted with a transition metal activator ($(M_t^i/L, L = \text{ligand})$) to generate the propagation radicals *R* (governed by an activation rate constant, k_{act}), then *R* reacted with the oxidized metal deactivator (K_p^{APP}) to reform the dormant alkyl halide species R-X (governed by a deactivation rate constant, k_{deact}). *R* could also propagate with monomer *M* (governed by a propagation rate constant, k_p) and terminate as in conventional free radical polymerization by either coupling or disproportionation (governed by a termination rate constant, k_t). The mechanism of normal ATRP is illustrated in Figure 1.

There are some drawbacks in normal ATRP such as the sensitivity of catalyst to air, the toxicity, and

high costs of ligands.³ These drawbacks have been overcome by the reverse ATRP (RATRP).^{4–6} In RATRP, the catalyst is added in its higher oxidation state instead of a lower oxidation state because the higher oxidation state is more soluble, thermally and air-stable, so this method would be more compatible with commercial process. Chains are activated by conventional radical initiator 2,2'-azobisisobutyronitrile (AIBN) and deactivated by transition metals. But, the amount of catalyst can not be reduced and block copolymers are always difficult to prepare by RATRP. To overcome these limitations, simultaneous reverse and normal initiation ATRP (SR&NI) was developed.^{7,8} In this process, AIBN is decomposed to generate radicals. The radicals are subsequently deactivated by higher oxidation state salt forming lower oxidation state salt and some halogenated chains. The latter can then reactivate ATRP initiator and concurrently mediate normal ATRP. The amount of catalyst can be reduced and block copolymers can be prepared. But the block copolymers are usually contaminated by a fraction of homopolymers formed through direct initiation from the added traditional initiator.

To prepare pure block polymers, recently, a new technique named activator generated by electron transfer (AGET) ATRP was developed.⁹ Instead of employing a conventional radical initiator to activate the catalyst complex as in "reverse" ATRP and SR&NI, In AGET ATRP, activators generated by electron transfer use a reducing agent to react with

Correspondence to: G. Wang (wangxwzl@163.com).

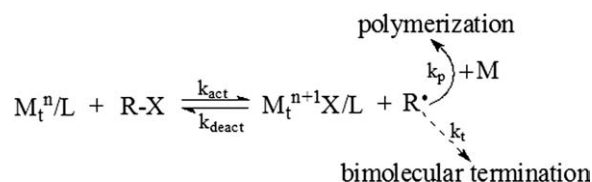


Figure 1 The mechanism of normal ATRP.

higher oxidation state salt to form active catalyst species that are unable to initiate new chains. Therefore, AGET ATRP has a significant advantage over “reverse” ATRP and SR&NI ATRP. AGET ATRP has been successfully applied to obtain well-defined polymers in organic media and heterogeneous systems. However, the amount of catalyst required in an AGET ATRP is generally in the range of 5000 ppm and postpurification procedures are required and also catalyst cannot be recycled for further use.

There are some other alternatives being developed to reduce the amount of catalyst, such as regenerating activator by electron transfer^{10–13} ATRP and initiators for continuous activator regeneration (ICAR) ATRP.¹⁴ Some transition metals, such as Cu,^{15,16} Fe,^{17–19} Ru,²⁰ and Ni,²¹ have been used in ATRP. The most extensively studied catalyst is copper. In comparison to copper, the iron-based catalyst is non-toxic, inexpensive, and environment-friendly. Sawamoto and Coworkers¹⁷ first reported that living radical polymerization of methyl methacrylate (MMA) was performed using iron(II) bis(triphenylphosphine)dichloride [FeCl₂(PPh₃)₂] with organic halides as initiators in the absence or presence of Al(OiPr)₃ in toluene at 80°C. Matyjaszewski et al.¹⁸ reported that controlled/“living” radical polymerization of styrene and methyl methacrylate was carried out using iron halide/4,4′-bis(5-nonyl)-2,2′-bipyridine, trialkylamines, triphenylphosphine, trialkylphosphines, and trialkylphosphites as catalysts. The polymerization rate and molecular weight distribution were affected by the structure of the coordinating ligands and the monomers employed. Some organic acids, such as isophthalic acid,²² iminodiacetic acid,²³ acetic acid,²⁴ succinic acid,²⁵ and lactic acid,²⁶ have been successfully employed as ligands in iron-mediated ATRP. The organic acids have some advantages such as nontoxicity and low costs.

To date, only a few iron-mediated ICAR ATRPs have been reported. Zhu et al.²⁷ reported that ICAR ATRP of MMA was carried out using FeCl₃·6H₂O/triphenylphosphine (PPh₃) as a catalyst, AIBN as a thermal radical initiator, and 1,4-(2-bromo-2-methylpropionato)benzene as an ATRP initiator. Polydispersities of the obtained polymers were around 1.37. The mechanism of iron-mediated ICAR ATRP is illustrated in Figure 2. The advantage of ICAR ATRP technique is that a tiny amount of catalyst is used and decreased to ppm level. Furthermore,

ICAR ATRP can probably be conducted in existing industrial equipment using thermal free radical initiators. However, the pure block copolymers did not yield due to the use of thermal free radical initiators, such as AIBN. To the best of the author’s knowledge, there is no report on iron-mediated ICAR ATRP using organic acids as ligands. In this study, ICAR ATRP of MMA was performed using FeCl₃·6H₂O/succinic acid as a catalyst, AIBN as a thermal radical initiator, and ethyl 2-bromoisobutyrate (EBiB) as an ATRP initiator.

EXPERIMENTAL

Materials

MMA was purchased from Tianjin Fuchen Chemical Reagents Factory, China. It was distilled under reduced pressure prior to use. EBiB (99%), obtained from Tianjin Alfa Aesar Chemical, China, was used without further purification. *N,N*-dimethylformamide (DMF), purchased from Tianjin Tianda Chemical Reagents Factory, China, was distilled under reduced pressure before use. AIBN, obtained from Sinopharm Chemical Reagent, Shanghai, China, was recrystallized from methanol. Ferric chloride hexahydrate was purchased from Shanghai Qingfeng Chemical Factory, China. Succinic acid was obtained from Wuhan Yinhe Chemical.

Polymerization

In the previous work, the ratio of the components has been optimized (unpublished results), so the result of optimal test was listed in this work. The ICAR ATRP of MMA was carried out based on the ratio of [MMA]₀/[EBiB]₀/[FeCl₃·6H₂O]₀/[SA]₀/[AIBN]₀ = 300/1/0.02/0.1/0.1 under nitrogen in 100-mL three-neck round-bottom flask equipped with magnetic stirring bar. A typical example of the general procedure is as follows: MMA (0.12 mol, 12 g), EBiB (4 × 10⁻⁴ mol, 0.078 g), FeCl₃·6H₂O (8 × 10⁻⁶ mol, 0.022 g), succinic acid (4 × 10⁻⁵ mol, 0.047 g), AIBN (4 × 10⁻⁵ mol, 0.066 g) and 20 mL DMF were added to the flask. The flask was then placed in an oil bath held by a thermostat at the desired reaction temperature to polymerize under

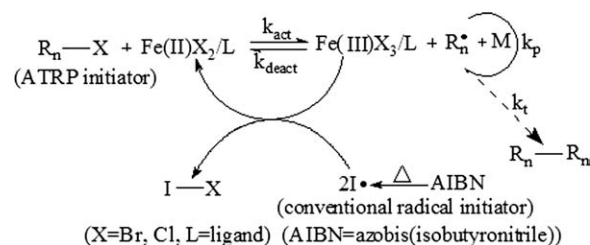


Figure 2 The mechanism of iron-mediated ICAR ATRP.

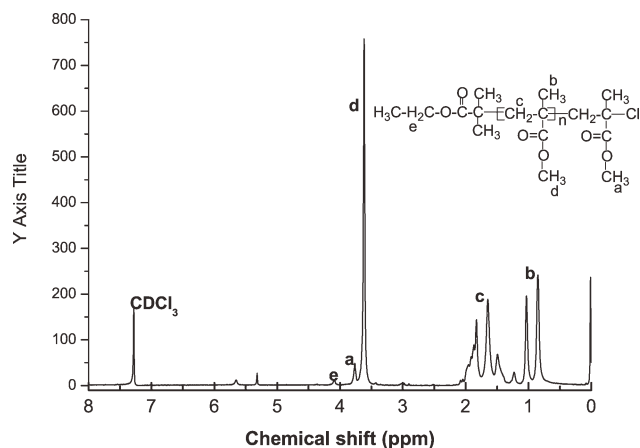


Figure 3 ¹H NMR spectrum of PMMA ($M_n = 14762$ g/mol, PDI = 1.25) prepared by ICAR ATRP at 90°C in DMF.

stirring. After the desired polymerization time, the flask was cooled by immersing into ice water. The reactant was pored into a large amount of methanol for precipitation. The obtained poly(methyl methacrylate) (PMMA) was vacuum-dried at 60°C for 1 day. Monomer conversion was determined by gravimetry.

Measurements

The number-average molecular weight ($M_{n,GPC}$) and polydispersities index (PDI) of the polymer were determined with a Waters 1515 gel permeation chromatography (GPC) equipped with refractive index detector, using HR1, HR3, and HR4 column with molecular weight range 100–500,000 calibrated with polystyrene standard sample. Tetrahydrofuran was used as a mobile phase at a flow rate of 1.0 mL/min and with column temperature of 30°C and polystyrene standards were used to calibrate the columns. The theoretical $M_{n(th)}$ of MMA can be calculated by the following equation:

$$M_{n(th)} = ([MMA]_0/[I]_0) \times W_{MMA} \times x \quad (1)$$

where, $[MMA]_0$ is the initial concentration of MMA, $[I]_0$ is the initial concentration of EBiB and W_{MMA} is the molecular weight of MMA, and x is the monomer conversion. ¹H NMR spectrum was recorded on a nuclear magnetic resonance (NMR) instrument (Bruker 400 MHz Spectrometer) using CDCl₃ as the solvent and tetramethylsilane as the internal standard at ambient temperature.

RESULTS AND DISCUSSION

¹H NMR spectrum

The ¹H-NMR spectrum of PMMA prepared by ICAR ATRP at 90°C is shown in Figure 3. The chemical

shift at 4.06 ppm belonged to the protons of the methylene (e in Fig. 3), which was the residue of initiator (EBiB) used in ATRP. This indicates that the moieties were successfully attached onto the chain end of the PMMA. The chemical shift at 3.78 ppm (a in Fig. 3) corresponded to the methoxy group next to the halogen chain end, as mentioned by Sawamoto.¹⁷ The chemical shift at 3.60 ppm was assigned to the protons of methoxy group in the main chain.¹⁷ The chemical shifts at 0.8–1.2 ppm (b in Fig. 3) and 1.4–2.0 ppm (c in Fig. 3) were attributed to the protons of methyl groups and methylene group, respectively.

ICAR ATRP of MMA catalyzed by FeCl₃·6H₂O/succinic acid

The ICAR ATRP of MMA was carried out at 90°C in DMF catalyzed by FeCl₃·6H₂O/succinic acid with the molar ratio of $[MMA]_0/[EBiB]_0/[FeCl_3 \cdot 6H_2O]_0/[SA]_0/[AIBN]_0 = 300/1/0.02/0.1/0.1$. As shown in Figure 4, the conversion increased with increasing reaction time, and the conversion reached 52.8 % within 72 h. A straight line of $\ln([M]_0/[M])$ versus reaction time was observed, indicating that the concentration of active species was constant during the course of polymerization and the polymerization obeyed first-order kinetics in monomer. This suggests that no termination reactions occurred during the polymerization process. The apparent rate constant K_p^{app} was $2.85 \times 10^{-6} \text{ s}^{-1}$ according to the slope of $\ln([M]_0/[M])$ versus reaction time in Figure 4.

Figure 5 shows the dependence of $M_{n,GPC}$ and PDI of the obtained PMMA versus monomer conversion. The $M_{n,GPC}$ increased from 12,342 to 31,664 g/mol with monomer conversion from 12.2 to 52.8 %. The $M_{n,GPC}$ was very close to the theoretical values, indicating a good control over the polymerization.

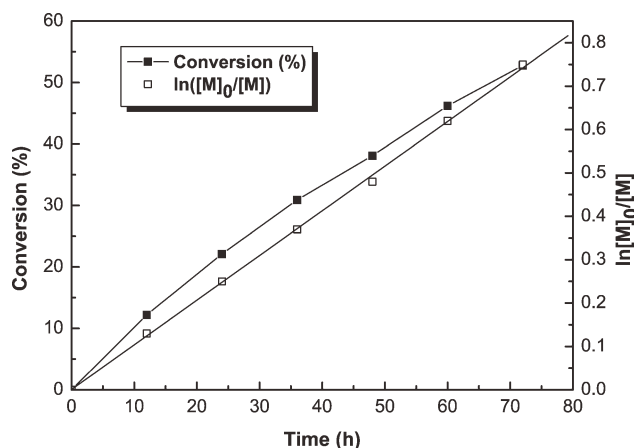


Figure 4 The kinetic plot for ICAR ATRP of MMA catalyzed by FeCl₃·6H₂O/SA at 90°C in DMF. The molar ratio is $[MMA]_0/[EBiB]_0/[FeCl_3 \cdot 6H_2O]_0/[SA]_0/[AIBN]_0 = 300/1/0.02/0.1/0.1$.

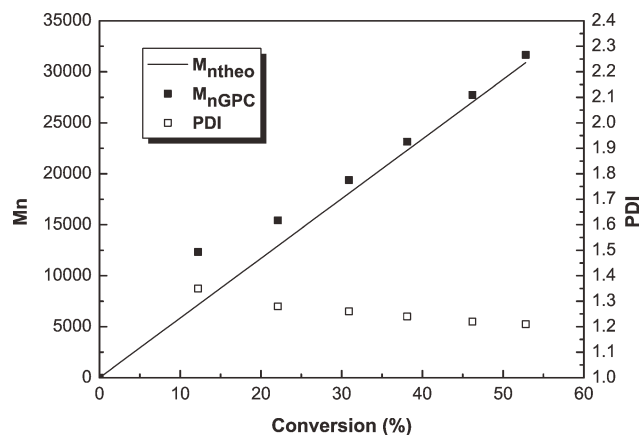


Figure 5 Dependence of M_n and PDI on monomer conversion for ICAR ATRP of MMA catalyzed by $\text{FeCl}_3 \cdot 6\text{H}_2\text{O}/\text{SA}$ at 90°C in DMF. The molar ratio is $[\text{MMA}]_0/[\text{EBiB}]/[\text{FeCl}_3 \cdot 6\text{H}_2\text{O}]/[\text{SA}]/[\text{AIBN}] = 300/1/0.02/0.1/0.1$.

Moreover, the values of PDI decreased from 1.35 to 1.21 with increasing monomer conversion from 12.2 to 52.8%, indicating that ICAR ATRP of MMA was a controlled radical polymerization. However, at the early stage of polymerization, the $M_{n,\text{GPC}}$ and PDI values were a little higher, this results suggested the possibility of coupling reactions of macroradical.

Effect of catalyst on polymerization

The catalyst plays an important role in ATRP since it controls the dynamic equilibrium between dormant species and propagating radicals. In order to investigate effect of catalyst on polymerization, a series of experiments were carried out with the molar ratio of $[\text{MMA}]/[\text{EBiB}]/[\text{AIBN}] = 300 : 1 : 0.1$. The concentration of Fe was 30, 67, and 100 ppm, respectively. As can be seen from Figure 6, the con-

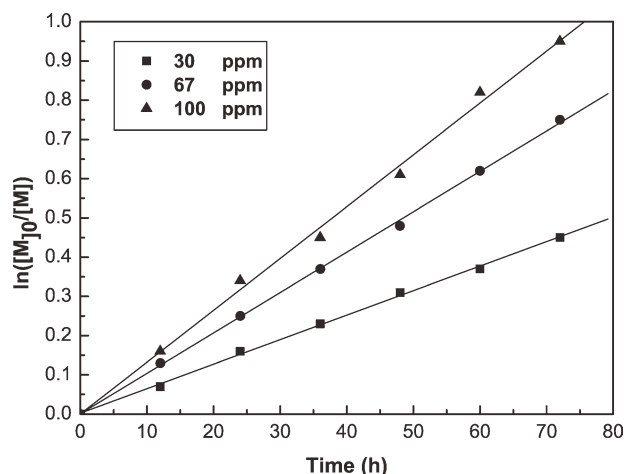


Figure 6 The kinetic plot for ICAR ATRP of MMA catalyzed by $\text{FeCl}_3 \cdot 6\text{H}_2\text{O}/\text{SA}$ at 90°C in DMF. The molar ratio is $[\text{MMA}]_0/[\text{EBiB}]_0/[\text{SA}]_0/[\text{AIBN}]_0 = 300/1/0.1/0.1$.

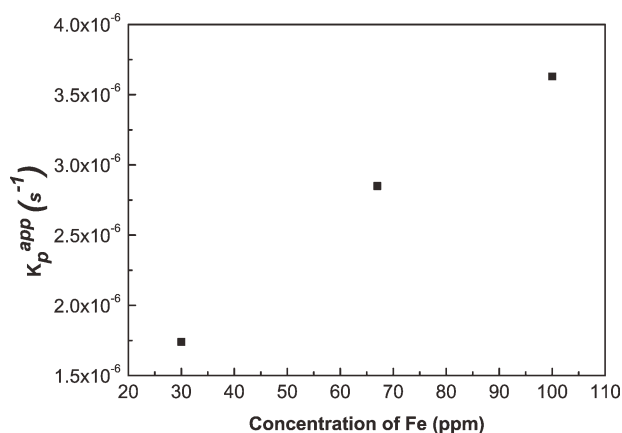


Figure 7 Effect of concentration of Fe on the apparent rate constant K_p^{app} .

centration of Fe had a great influence on the ICAR ATRP of MMA. The kinetic plot of $\ln([\text{M}]_0/[\text{M}])$ versus time was linear throughout the reaction. The polymerization rate increased with the increase of Fe concentration. The apparent rate constant K_p^{app} was 1.74 , 2.85 , and $3.63 \times 10^{-6} \text{ s}^{-1}$, respectively. Figure 7 shows effect of concentration of Fe on the polymerization. As shown in Figure 7, increasing the concentration of Fe resulted in an increase in the polymerization rate.

The dependence of $M_{n,\text{GPC}}$ and PDI of the polymers on the monomer conversion was studied at various concentration of Fe. As shown in Figure 8, the $M_{n,\text{GPC}}$ increased with increasing monomer conversion and were in good agreement with the theoretical values, indicated that all the reactions proceeded in a controlled way. The PDI values of the polymers decreased with increasing monomer conversion, and the values of PDI were less than 1.3 with 67 and 100 ppm. The values of PDI were broad with 30 ppm, which can be attributed to the lower concentration of Fe species and slow deactivation.

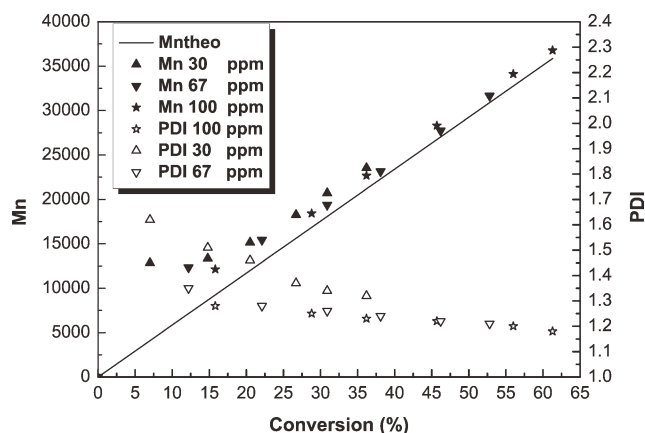


Figure 8 Dependence of M_n and PDI on monomer conversion for ICAR ATRP of MMA catalyzed by $\text{FeCl}_3 \cdot 6\text{H}_2\text{O}/\text{SA}$ at 90°C in DMF. The molar ratio is $[\text{MMA}]_0/[\text{EBiB}]_0/[\text{SA}]_0/[\text{AIBN}]_0 = 300/1/0.1/0.1$.

TABLE I
Effect of Concentration of AIBN on ICAR ATRP of MMA at 90 °C in DMF with [MMA]/[EBiB]₀/[FeCl₃·6H₂O]₀/[SA]₀ = 300 : 1 : 0.02/0.1

Entry	R ^a	Time (h)	Conversion (%)	M _{n,th} (g/mol)	M _{n,GPC} (g/mol)	PDI
1	300 : 1 : 0.02 : 0.1 : 0.1	36	36.4	21229	22513	1.22
2	300 : 1 : 0.02 : 0.1 : 0.3		44.5	26039	26817	1.23
3	300 : 1 : 0.02 : 0.1 : 0.5		48.7	29497	31087	1.36

$$R^a = [\text{MMA}]_0/[\text{EBiB}]_0/[\text{FeCl}_3\cdot 6\text{H}_2\text{O}]_0/[\text{SA}]_0/[\text{AIBN}]_0.$$

At the beginning of polymerization, the deviation between $M_{n,GPC}$ and $M_{n,th}$ indicated the coupling reaction, the suggestion was demonstrated by the higher PDI values.

Effect of AIBN concentration on polymerization

In typical ICAR ATRP system, a conventional radical initiator AIBN is used as the reducing agent. To further investigate effect of AIBN concentration of on polymerization, a series of experiments were carried out with various amount of AIBN, and the results are shown in Table I.

The role of AIBN as a reducing agent in the polymerization was also studied. The polymerization conversion increased from 36.4 to 48.7% when the ratio of AIBN ranged from 0.1 to 0.5, indicating that AIBN had a great influence on the polymerization. In ICAR ATRP system, the Fe (III) complex is reduced to Fe (II) complex via AIBN. The amount of Fe (II) complex increased with increase of AIBN. The $M_{n,GPC}$ increased from 21,229 to 29,497 g/mol with ratio of AIBN from 0.1 to 0.5. The $M_{n,GPC}$ was very close to the theoretical values. However, the value of PDI was broad when the ratio of AIBN was 0.5, due to the increase of side reactions with the increasing ratio of AIBN.

Chain extension of PMMA

The living nature of iron-mediated ICAR ATRP system was confirmed by chain extension. The obtained PMMA ($M_{n,GPC} = 14,672$ g/mol, PDI = 1.27) with an ω-chlorine end group can be used as a macroinitiator for chain extension polymerization. The chain extension of PMMA was carried out at 90°C in DMF, with the molar ratio of [MMA]₀/[EBiB]₀/[FeCl₃·6H₂O]₀/[SA]₀/[AIBN]₀ = 300/1/0.02/0.1/0.1. Figure 8 displays the GPC curves of the macroinitiator, chain-extended PMMA. After chain extension, the GPC curves clearly shifted to high molecular weight. Although the PDI of the resultant PMMA were higher than that of the macroinitiator, they provided other evidence for the well-defined structure of PMMA having an active chlorine-terminated group. No macroinitiator can be observed from Figure 9 in the GPC traces of extended PMMA,

implying that the chlorine group was indeed present for about 100% after ICAR ATRP of MMA.

CONCLUSION

In this study, an environmentally friendly Fe catalyst complex system was developed. ICAR ATRP of MMA has been successfully carried out using FeCl₃·6H₂O/succinic acid as catalyst, EBiB as ATRP initiator and AIBN as thermal radical initiator. Comparing to traditional ATRP, the amount of Fe catalyst decreased to a level of ppm in ICAR ATRP, decreasing the amount of catalyst resulted in decreasing the metal residue in the final product. This technique would be attractive potential for its application in industrial scale. Although tiny amount of catalyst used, the polymerization was demonstrated to be a controlled/"living" process with controlled molecular weights and low PDI according to GPC analyses. It indicated that the catalyst system can be efficiently used for the ICAR ATRP of MMA. The kinetics study showed a linear relationship between ln([M]₀/[M]) and reaction time, indicating the "living/controlled" feature of polymerization with ppm level of catalyst. The polymerization rate increased with increasing the amount of catalyst and AIBN. The presence of a ω-Cl end group on the obtained

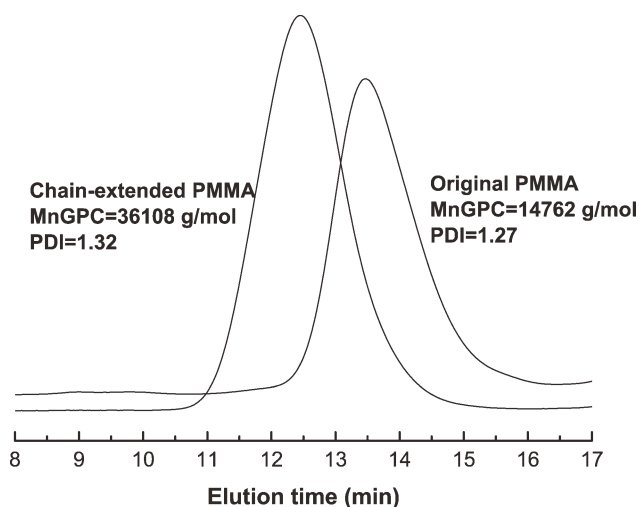


Figure 9 GPC curves of PMMA before and after chain extension via ICAR ATRP at 90°C in DMF.

polymer chain was determined by ^1H NMR. The living feature was further verified by chain extension of PMMA macroinitiators.

The authors are grateful to Yong Gao and Yu Liu, Xiangtan University, for their assistance in GPC and NMR analyses.

References

1. Kato, M.; Kamigaito, M.; Sawamoto, M.; Higashimura, T. *Macromolecules* 1995, 28, 1721.
2. Wang, J. S.; Matyjaszewski, K. *J Am Chem Soc* 1995, 117, 5614.
3. Islam, M.; Mondal, P.; Roy, A. S.; Tuhina, K. *Transit Metal Chem* 2010, 35, 491.
4. Wang, J. S.; Matyjaszewski, K. *Macromolecules* 1995, 28, 7572.
5. Xia, J.; Matyjaszewski, K. *Macromolecules* 1997, 30, 7692.
6. Moineau, G.; Dubois, P.; Jérôme, R.; Senninger, T.; Teyssié, P. *Macromolecules* 1998, 31, 545.
7. Gromada, J.; Matyjaszewski, K. *Macromolecules* 2001, 34, 7664.
8. Li, M.; Jahed, N. M.; Min, K.; Matyjaszewski, K. *Macromolecules* 2004, 37, 2434.
9. Jakubowski, W.; Matyjaszewski, K. *Macromolecules* 2005, 38, 4139.
10. Burdyńska, J.; Cho, H. Y.; Mueller, L.; Matyjaszewski, K. *Macromolecules* 2010, 43, 9227.
11. Dong, H.; Matyjaszewski, K. *Macromolecules* 2008, 41, 6868.
12. Matyjaszewski, K.; Dong, H.; Jakubowski, W.; Pietrasik, J.; Kusumo, A. *Langmuir* 2007, 23, 4528.
13. Min, K.; Gao, H.; Matyjaszewski, K. *Macromolecules* 2007, 40, 1789.
14. Mueller, L.; Jakubowski, W.; Tang, W.; Matyjaszewski, K. *Macromolecules* 2007, 40, 6464.
15. Tsarevsky, N. V.; Matyjaszewski, K. *Chem Rev* 2007, 107, 2270.
16. Pintauer, T.; Matyjaszewski, K. *Coord Chem Rev* 2005, 249, 1155.
17. Ando, T.; Kamigaito, M.; Sawamoto, M. *Macromolecules* 1997, 30, 4507.
18. Matyjaszewski, K.; Wei, M.; Xia, J.; McDermott, N. E. *Macromolecules* 1997, 30, 8161.
19. Luo, R.; Sen, A. *Macromolecules* 2008, 41, 4514.
20. Plichta, A.; Li, W.; Matyjaszewski, K. *Macromolecules* 2009, 42, 2330.
21. Griffith, B. R.; Allen, B. L.; Rapraeger, A. C.; Kiessling, L. L. *J Am Chem Soc* 2004, 126, 1608.
22. Zhu, S.; Yan, D. *Macromolecules* 2000, 33, 8233.
23. Zhang, L.; Cheng, Z.; Shi, S.; Li, Q.; Zhu, X. *Polymer* 2008, 49, 3054.
24. Zhu, S.; Yan, D.; Zhang, G. *Polym Bull* 2001, 45, 457.
25. Zhu, S.; Yan, D.; Zhang, G.; Li, M. *Macromol Chem Phys* 2000, 201, 2666.
26. Xiong, Y.; Fan, L.; Shen, Z. *Chem J Chin Univ (in Chinese)* 2005, 26, 2153.
27. Zhu, G.; Zhang, L.; Zhang, Z.; Zhu, J.; Tu, Y.; Cheng, Z.; Zhu, X. *Macromolecules* 2011, 44, 3233.